

A “breathing” octupole ^{208}Pb nucleus: resolving the elliptical-to-triangular azimuthal anisotropy puzzle in ultracentral relativistic heavy ion collisions

Hao-jie Xu,^{1,2,*} Duoduo Xu,³ Shujun Zhao,³ Wenbin Zhao,^{4,5} Huichao Song,^{3,6,7} and Fuqiang Wang⁸

¹*School of Science, Huzhou University, Huzhou, Zhejiang 313000, China*

²*Strong-Coupling Physics International Research Laboratory (SPiRL),
Huzhou University, Huzhou, Zhejiang 313000, China.*

³*School of Physics, Peking University, Beijing 100871, China*

⁴*Nuclear Science Division, Lawrence Berkeley National Laboratory, Berkeley, California 94720, USA*

⁵*Physics Department, University of California, Berkeley, California 94720, USA*

⁶*Collaborative Innovation Center of Quantum Matter, Beijing 100871, China*

⁷*Center for High Energy Physics, Peking University, Beijing 100871, China*

⁸*Department of Physics and Astronomy, Purdue University, West Lafayette, Indiana 47907, USA*

Relativistic heavy ion collisions provide a unique opportunity to probe the nuclear structure by taking an instantaneous snapshot of the colliding nuclei and converting it into momentum anisotropies of final emitted hadrons. A long-standing puzzle of too large a ratio of the elliptical-to-triangular (v_2 -to- v_3) anisotropies in ultracentral $^{208}\text{Pb}+^{208}\text{Pb}$ collisions at the Large Hadron Collider(LHC) cannot be solved simply by hydrodynamic simulations with initial conditions containing the spherical or certain deformed shape of ^{208}Pb . In this Letter, using the iEBE-VISHNU relativistic viscous hydrodynamic hybrid model simulations with the TRENTo initial condition, we show that a dynamic octupole deformation—a shape-breathing of ^{208}Pb —could potentially solve the v_2 -to- v_3 puzzle and simultaneously describe the $v_3\{4\}$ data measured in experiment. Our results highlight the unique capability of capturing transient collective properties of nuclei on yoctosecond (10^{-24} s) timescales, unfeasible with low-energy nuclear reactions.

Introduction. Relativistic heavy ion collisions at the Relativistic Heavy Ion Collider (RHIC) and the Large Hadron Collider (LHC) aim to create and study the quark-gluon plasma (QGP), a deconfined state of strongly interacting matter that once existed in the very early universe shortly after the big bang [1–10]. Within the hydrodynamic framework, the pressure gradient of the QGP converts the spatial anisotropy of the initial overlapping geometry of the colliding nuclei into momentum anisotropy of final-state hadrons, called collective flow [11, 12]. The flow anisotropies are expressed by Fourier harmonics in the azimuthal (ϕ) distribution of final-state particles relative to the reaction planes (ψ_n) [13],

$$\frac{dN}{d\phi} \propto 1 + \sum_{n=1} 2v_n \cos n(\phi - \psi_n). \quad (1)$$

The success of relativistic hydrodynamics in modeling the evolution of the QGP establishes a robust connection between the initial geometry eccentricities and the final-state momentum anisotropies with $v_n \propto \epsilon_n$ for ($n=2,3$) [14–22].

For ultracentral collisions of spherical nuclei at relativistic energies, the initial geometry anisotropies are predominantly driven by fluctuations, yielding comparable values, for example, for the second- and third-order eccentricities $\epsilon_2 \approx \epsilon_3$ [23]. Because the viscous damping effects are stronger for higher-order cumulants, hydrodynamic models predict a smaller triangular flow than the elliptic flow, $v_3 < v_2$ [23]. The predicted v_2/v_3 ratio is then too large compared to the measurements in ultracentral $^{208}\text{Pb}+^{208}\text{Pb}$ collisions at $\sqrt{s_{\text{NN}}} = 2.76$ TeV and 5.02 TeV [24–28]. This discrepancy, known as the “ultracentral v_2 -to- v_3 puzzle,” has been a long-standing challenge in heavy ion physics for over a decade.

Nuclear structure has become a vital aspect in relativistic

heavy-ion collisions, for example, in elucidating background contributions to the chiral magnetic effect in isobar collisions [29–31] and in resolving the ultracentral v_2 issue in $^{238}\text{U}+^{238}\text{U}$ collisions [32, 33]. An obvious possibility for the anomalously large v_3/v_2 ratio is that the doubly magic ^{208}Pb nucleus is octupole-deformed [34–36], with a finite β_3 value in the Woods-Saxon (WS) parameterization of nuclear density,

$$\rho(r) = \frac{\rho_0}{1 + \exp\left(\frac{r-R}{a}\right)}, \quad (2a)$$

$$R = R_0 (1 + \beta_2 Y_{20} + \beta_3 Y_{30}). \quad (2b)$$

Here, R_0 is the nuclear radius parameter, a is the diffuseness parameter, β_2 and β_3 quantify quadrupole and octupole deformations, respectively, and Y_{lm} denotes the spherical harmonics. In ultracentral collisions, the collision overlap geometry is determined essentially by the shape of the colliding nuclei, i.e. $\epsilon_n^2 \propto \beta_n^2$ (for $n=2,3$) [37, 38]. Since v_n is proportional to ϵ_n on the leading order, $v_n^2 \propto \beta_n^2$ [38–40]. A nonzero β_3 would, therefore, enhance v_3 and solve the v_2 -to- v_3 puzzle in ultracentral Pb+Pb collisions. However, the nonzero β_3 value fails to describe the observed $v_3\{4\}/v_3\{2\}$ ratio [34]. Here $v_n\{m\}$ is the n -th order flow harmonics calculated with m -particle cumulant method [41–43].

In this Letter, we solve the v_2 - v_3 puzzle by introducing β_3 fluctuation, which implies that the colliding ^{208}Pb nucleus “breathes” in a pear shape. The idea is as follows. It is known that $v_n\{2\}$ and $v_n\{4\}$ are sensitive to fluctuations but in different ways; $v_n\{2\}$ measures $\sqrt{\langle v_n^2 \rangle}$ and is thus sensitive to $\langle \beta_n^2 \rangle \equiv \langle \beta_n \rangle^2 + \sigma_{\beta_n}^2$, whereas the fluctuation effect in $v_n\{4\}$ is negative, approximately determined by $\langle \beta_n \rangle^2 - \sigma_{\beta_n}^2$.

The fact that, with a finite fixed β_3 value (i.e. $\sigma_{\beta_3} = 0$), the $v_3\{2\}/v_2\{2}$ ratio is described, but not the $v_3\{4\}/v_3\{2}$ ratio suggests that the fixed β_3 value correctly reflects $\langle\beta_3^2\rangle$, but the finite-number fluctuations are insufficient. With this consideration, the path to solve the v_2 -to- v_3 puzzle is clear: to enhance $v_3\{2\}$ nonzero $\langle\beta_3^2\rangle$ should be invoked; to describe the measured $v_3\{4\}/v_3\{2}$, the β_3 value should be allowed to fluctuate to introduce extra fluctuations beyond the stochastic nucleon positions.

Such breathing modes are consistent with the findings in low-energy nuclear structure studies [44–48]. ^{208}Pb stands as a benchmark nucleus in nuclear physics, playing a pivotal role in advancing our understanding of symmetry energy, a critical component of the nuclear equation of state [49–53]. As a doubly magic nucleus, with closed proton and neutron shells, ^{208}Pb exhibits exceptional stability, enabling clear observation of collective excitations like the giant monopole resonance (GMR), often termed the “breathing mode”, where the nucleus uniformly expands and contracts [54, 55]. Beyond this fundamental mode, Pb also displays higher-order vibrational modes, such as quadrupole ($L=2$) and octupole ($L=3$) resonances, which manifest as more complex, shape-driven oscillations [44–48]. These modes, interpreted as higher-order “breathing” behaviors, strongly suggest that the intrinsic shapes of doubly magic nuclei such as ^{208}Pb must be described dynamically with the mixing of different shape configurations [46, 48].

Model and setups. In previous studies, the nuclear shape parameters, i.e. β_2 and β_3 , are often treated as *fixed* values, and the position of nucleons are then sampled according to Eqs. (2). To investigate the octupole breathing mode, the β_3 fluctuations in ^{208}Pb are modeled by a Gaussian probability distribution in β_3 [44, 48],

$$P(\beta_3) \propto \exp\left[-\frac{(\beta_3 - \langle\beta_3\rangle)^2}{2\sigma_{\beta_3}^2}\right]. \quad (3)$$

Note that there is a similar distribution along the negative direction from the symmetry-conserving mixing method shown in Ref. [48], while the sign of β_3 is degenerate because $v_3\{2\}$ is sensitive only to the variance of the octupole deformation $\langle\beta_3^2\rangle$.

For the following calculations, we use the *iEBE-VISHNU* hybrid model [56, 57] to simulate relativistic Pb+Pb collisions at $\sqrt{s_{\text{NN}}} = 5.02$ TeV. The model contains three main components: initial conditions generated via the *TRENTO* model [58, 59]; the QGP evolution modeled with relativistic viscous hydrodynamics of $(2+1)$ dimension (*VISH2+1*) [60–62]; and late stage hadronic interactions simulated with the *UrQMD* hadron cascade model [63, 64]. All model parameters are taken from Ref. [65], calibrated for non-central Pb+Pb collisions at $\sqrt{s_{\text{NN}}} = 5.02$ TeV [66, 67] without considering the nuclear deformation and neutron skin of ^{208}Pb . Ultimately, a Bayesian calibration is required to extract shape deformation and fluctuation parameters as well as transport properties such as the specific shear viscosity from the data of soft physics in Pb+Pb collisions. We leave such a work to the future; Here, we

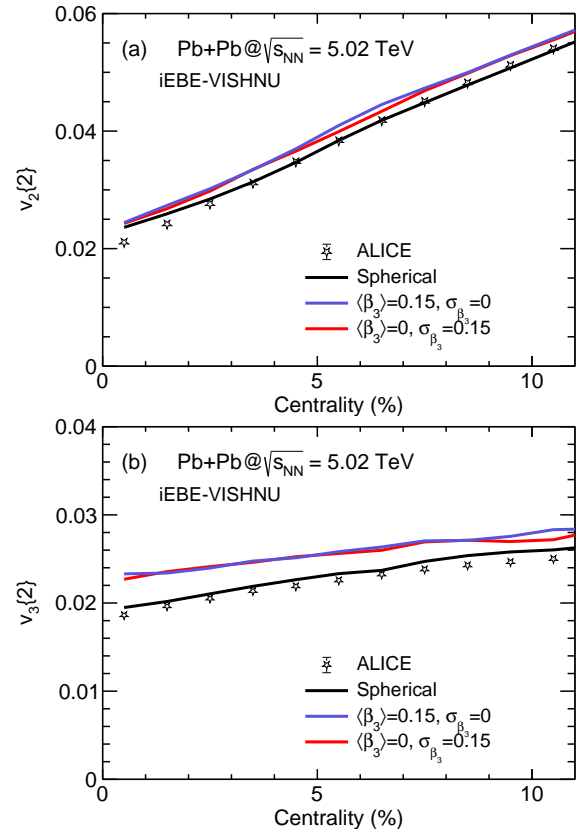


FIG. 1. (Color online) (a) The $v_2\{2\}$ and $v_3\{2\}$ at midrapidity in the most central Pb+Pb collisions at $\sqrt{s_{\text{NN}}} = 5.02$ TeV, calculated from *iEBE-VISHNU* hybrid model with three initial Woods-Saxon geometries, together with a comparison to the data from ALICE with $|\eta| < 0.8$ [27].

aim at a qualitative description of the data with the breathing mode of the colliding nuclei.

Results and discussions. In the following calculations, we firstly focus on three cases of the colliding nuclei: (i) spherical case without any deformation, (ii) a static/rigid pear-shaped ^{208}Pb with $\langle\beta_3\rangle = 0.15$ and $\sigma_{\beta_3} = 0$ and (iii) a “breathing” ^{208}Pb , spherical-shaped on average fluctuating into oppositely oriented pear shapes with $\langle\beta_3\rangle = 0$ and $\sigma_{\beta_3} = 0.15$. Figure 1 shows predictions for individual v_2 and v_3 in central Pb+Pb collisions at $\sqrt{s_{\text{NN}}} = 5.02$ TeV. The calibrated Bayesian parameters for a spherical ^{208}Pb case (i), can accurately describe both $v_2\{2\}$ and $v_3\{2\}$, except for the top 2% centrality. Resolving the v_2 -to- v_3 ratio will require different relative changes to v_2 and v_3 . This is achieved by case (ii) and (iii), though the individual v_2 and v_3 magnitudes are overpredicted. The v_2 and v_3 magnitudes can be simultaneously tuned—for example, by adjusting bulk properties, nucleon width, or the minimum separation distance between nucleons in the colliding nuclei [68].

Figure 2 shows the $v_2\{2\}/v_3\{2\}$ ratio in the most central Pb+Pb collisions, calculated from *iEBE-VISHNU*. Although the individual v_2 and v_3 was overestimated, both cases (ii) and (iii) generate an enhanced magnitude of $v_3\{2\}$, which could solve the v_2 -to- v_3 ratio puzzle in ultracentral collisions. This

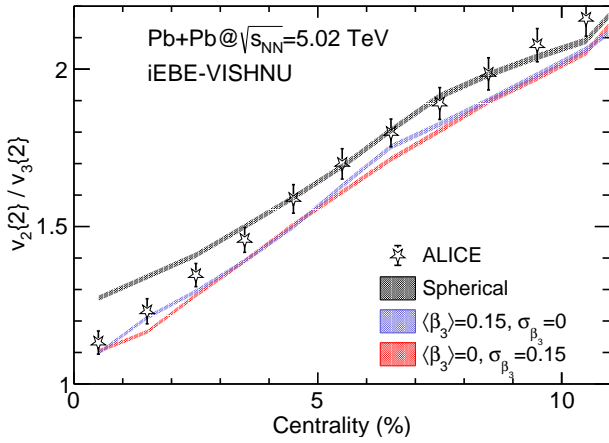


FIG. 2. (Color online) Similar to Fig 1 but for the $v_2\{2\}/v_3\{2\}$ ratios at midrapidity in the most central Pb+Pb collisions at $\sqrt{s_{NN}} = 5.02$ TeV. The widths of the bands indicate statistical uncertainties of the calculations.

result is expected because the two-particle cumulant $v_3\{2\}$ is determined only by $\langle\beta_3^2\rangle = \langle\beta_3\rangle^2 + \sigma_{\beta_3}^2$, which is equivalence in these two cases.

Such an ambiguity in the two-particle cumulants can be resolved by the four-particle cumulants as briefly discussed above. However, the associated full hydrodynamic calculations are computationally expensive. Considering that the linear relationship between the final-state flow anisotropy and the initial-state eccentricity, $v_n \propto \epsilon_n$ for $n = 2, 3$ in the most central collisions [39, 40], we calculate the eccentricity cumulants as a function of centrality with the TRENTo initial-state model. Figure 3 shows the calculated ratios, $-c_{2,\epsilon}\{4\}/c_{2,\epsilon}\{2\}^2$ and $-c_{3,\epsilon}\{4\}/c_{3,\epsilon}\{2\}^2$, together with a comparison to the ALICE measurements $-c_2\{4\}/c_2\{2\}^2$ and the ATLAS measurements $-c_3\{4\}/c_3\{2\}^2$. Overall, the results from spherical nucleus are consistent with data (we have also verified that the residual discrepancy in $-c_{2,\epsilon}\{4\}/c_{2,\epsilon}\{2\}^2$ disappears once final-state effects from hydrodynamics are considered). This is an accident because the spherical nucleus case cannot describe the anomalously large v_3/v_2 ratio. The data do not require a quadrupole (prolate or oblate) deformation of a finite β_2 . As expected, octupole deformation, with or without breathing, also does not affect the quadrupole cumulants. On the other hand, octupole deformation directly affects ϵ_3 (and hence v_3), as shown in Fig. 3(b). Neither the static deformed nor the breathing nucleus can describe the $-c_{3,\epsilon}\{4\}/c_{3,\epsilon}\{2\}^2$ data. A striking consequence of the “breathing” mode of ^{208}Pb is to drive $-c_3\{4\}$ to significantly negative values in ultracentral.

In order to identify the degree of octupole breathing of the ^{208}Pb nucleus, we compare final-state hydrodynamic calculations to data measurements. The four-particle cumulants in Pb+Pb collisions have been published by ALICE for $c_2\{4\}$ in the top 1% centrality [27] and by ATLAS for $c_3\{4\}$ in the top 2% centrality [28]. To enhance ultracentral 0–2% collisions, we run full hydrodynamic simulations by iEBE-VISHNU with restricted impact parameter range of $b < 4$ fm, and then use

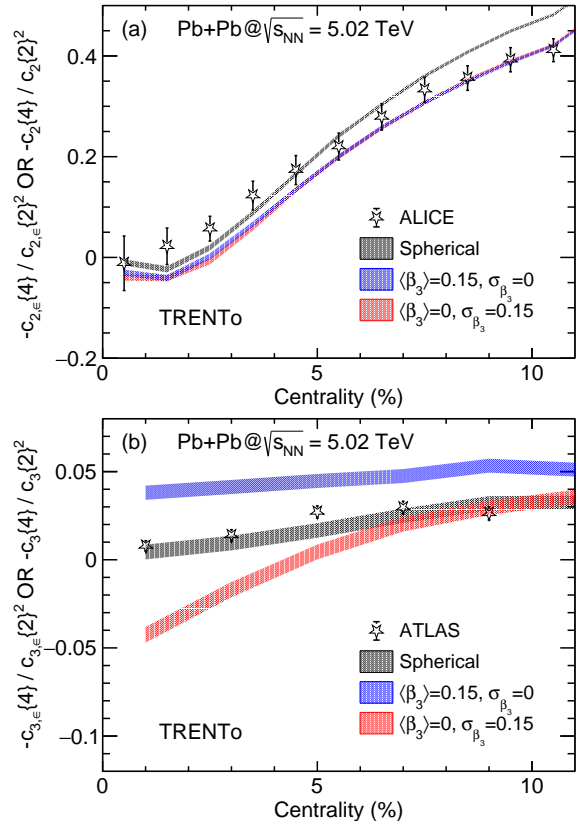


FIG. 3. (Color online) Four-particle cumulants in the most central Pb+Pb collisions at $\sqrt{s_{NN}} = 5.02$ TeV, calculated from initial-state model TRENTo with three initial geometries as used in Fig. 2. (a) $-c_{2,\epsilon}\{4\}/c_{2,\epsilon}\{2\}^2$, compared to $-c_2\{4\}/c_2\{2\}^2$ from ALICE [27] with $|\eta| < 0.8$, and (b) $-c_{3,\epsilon}\{4\}/c_{3,\epsilon}\{2\}^2$, compared to $-c_3\{4\}/c_3\{2\}^2$ from ATLAS [28] with $|\eta| < 2.5$.

the charged-hadron multiplicity to determine our centrality percentage (relative to minimum bias sample). Figure 4 shows in (a) $v_2\{4\}/v_2\{2\}$ within $p_T > 0.2$ GeV/c in the top 0–1% centrality compared to ALICE data, and in (b) $v_3\{4\}/v_3\{2\}$ within $p_T > 0.5$ GeV/c in the top 0–2% centrality compared to ATLAS data. We note that the parameter set used in this work is calibrated using anisotropic flow data as functions of centrality from ALICE [65–67]; The calculated $v_2\{2\}/v_3\{2\}$ values are slightly overestimated compared to ATLAS data. In addition, the $(2 + 1)$ dimension hydrodynamic model employed in this study may lack certain characteristics, such as longitudinal flow decorrelation over a wide pseudo-rapidity range, that may be important for the ATLAS data.

The v_2/v_3 ratio is equally reproduced by the two scenarios, static deformation and shape fluctuations. The spherical nucleus case ($\beta_3 = 0$) is ruled out. Although statistical uncertainties are large for the 0–1% centrality, the $c_2\{4\}/c_2\{2\}^2$ appears insensitive to σ_{β_3} , as expected. On the contrary, $c_3\{4\}/c_3\{2\}^2$ shows a strong sensitivity to β_3 deformation and fluctuations, mirroring trends in the initial-state TRENTo simulations (Fig. 3). Quantitatively, the final-state ratio exhibits an enhanced sensitivity, suggesting a breakdown of the

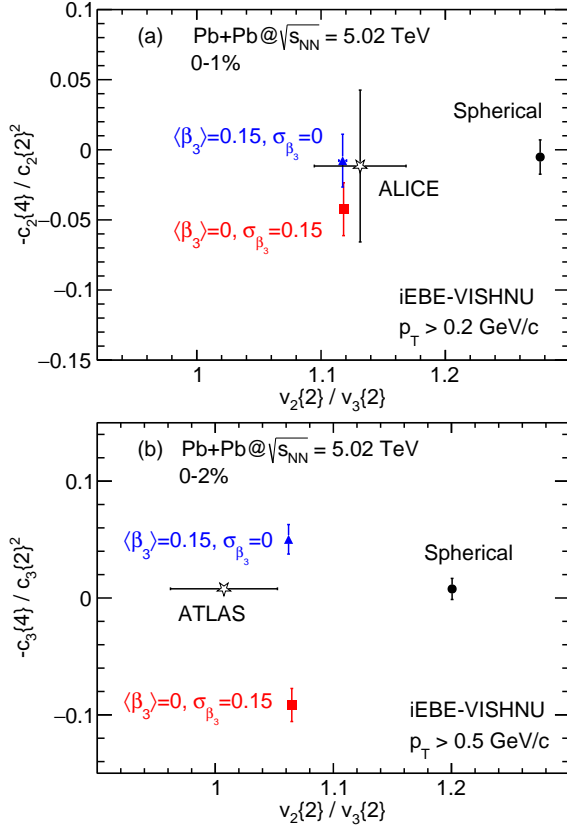


FIG. 4. (Color online) (a) $-c_2\{4\}/c_2\{2\}^2$ vs. $v_2\{2\}/v_3\{2\}$ in the top 1% centrality Pb+Pb collisions at $\sqrt{s_{NN}} = 5.02$ TeV, calculated from iEBE-VISHNU model with three initial geometries are used as in Fig. 2, together with a comparison to the ALICE data [27], and (b) $-c_3\{4\}/c_3\{2\}^2$ vs. $v_2\{2\}/v_3\{2\}$ in the top 2% centrality, together with a comparison to the ATLAS data [28].

simplistic mapping from initial- to final-state cumulants when shape fluctuations are involved.

As we have demonstrated in Fig. 4, the v_2 -to- v_3 puzzle in ultracentral Pb+Pb collisions can be equally solved by introduce a static or breathing octupole deformation of ^{208}Pb . In fact, it can be solved by any combination of the static octupole deformation $\langle\beta_3\rangle$ and dynamic fluctuations σ_{β_3} satisfying

$$\sqrt{\langle\beta_3^2\rangle} \equiv \sqrt{\langle\beta_3\rangle^2 + \sigma_{\beta_3}^2} = 0.15. \quad (4)$$

We now explore this by taking several combinations of $\langle\beta_3\rangle$ and σ_{β_3} that satisfying Eq.(6), using the initial-state quantities that are computationally efficient. In Fig. 5, we plots ϵ as a function of $\langle\beta_3\rangle^2$ in ultracentral 0–1% Pb+Pb collisions at $\sqrt{s_{NN}} = 5.02$ TeV, calculated by the initial-state TRenTo model (open blue points), together with the final-state iEBE-VISHNU simulations for the two limiting cases with $\sigma_{\beta_3}^2 = 0$ and 0.15 labeled by the extra right axis (the values of the two axes correspond to each other with the linear relationship $v_n \propto \epsilon_n$ for $n=2,3$). The experimental $v_2\{2\}/v_3\{2\}$ data with error bars (gray band on the extra right axis)

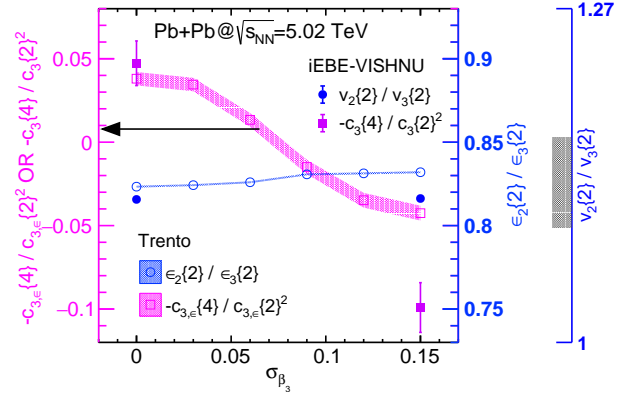


FIG. 5. (Color online) $c_{3,\epsilon}\{4\}/c_{3,\epsilon}\{2\}^2$ and $c_{2,\epsilon}\{4\}/c_{2,\epsilon}\{2\}^2$ in ultracentral 0–1% Pb+Pb collisions at $\sqrt{s_{NN}} = 5.02$ TeV calculated by the initial-state TRenTo model (open points) for various combinations of $\langle\beta_3\rangle$ and σ_{β_3} satisfying $\sqrt{\langle\beta_3\rangle^2 + \sigma_{\beta_3}^2} = 0.15$. The solid points are from the final-state iEBE-VISHNU simulations for the two limiting cases with $\sigma_{\beta_3}^2 = 0$ and 0.15. The blue band on the extra right axis denotes the $v_2\{2\}/v_3\{2\}$ data from ALICE (0–1% centrality) [27], and the red arrow on the left axis denotes the $-c_3\{4\}/c_3\{2\}^2$ data from ATLAS (0–2% centrality) [28].

be well reproduced. This implies that two-particle cumulant alone cannot distinguish the dynamic shape fluctuations from the static nuclear deformation of the colliding nuclei ^{208}Pb .

The degeneracy can be lifted by the four-particle cumulant. In Fig. 5, we also plot the initial-state ratio $c_{3,\epsilon}\{4\}/c_{3,\epsilon}\{2\}^2$ calculated from TRenTo with various combinations of $\langle\beta_3\rangle$ and σ_{β_3} (violet open points), and the final-state ratio $c_3\{4\}/c_3\{2\}^2$ calculated from iEBE-VISHNU for the two limiting cases (the violet solid points). The four-particle cumulant ratios exhibit obvious sensitivity on σ_{β_3} . Assuming a smooth correspondence from $c_{3,\epsilon}\{4\}/c_{3,\epsilon}\{2\}^2$ to $c_3\{4\}/c_3\{2\}^2$, the ATLAS data (arrow on the left vertical axis) prefers that the colliding nuclei ^{208}Pb is in a octupole breathing mode with a root-mean-square amplitude $\sigma_{\beta_3} \sim 0.06$ and the corresponding average octupole deformation is $\langle\beta_3\rangle \sim 0.14$. This result is consistent with nuclear structure calculations from self-consistent configuration mixing and multidimensional generator coordinate method [47, 48]. However, we also emphasize that these values of octupole breathing should not be taken as precise extraction at current stage, but a qualitative imaging of ^{208}Pb obtained from relativistic heavy ion collisions.

Summary and outlook. Relativistic heavy ion collisions take an instantaneous *snapshot* of the overlap interaction zone of the two colliding nuclei and convert it by strong interactions in the created quark-gluon plasma into momentum anisotropies in the final state. The elliptical-to-triangular (v_2 -to- v_3) anisotropic flow ratio in ultracentral $^{208}\text{Pb}+^{208}\text{Pb}$ collisions at the Large Hadron Collider was found to be too small compared hydrodynamic simulations with initial conditions containing the spherical shape of the colliding nuclei ^{208}Pb . This puzzle itself can be solved by introducing a pure static

octupole deformation ($\langle\beta_3\rangle = 0.15$ with $\sigma_{\beta_3} = 0$), a pure fluctuating octupole ($\langle\beta_3\rangle = 0$ with $\sigma_{\beta_3} = 0.15$), or anything in between. In this paper, we demonstrated that such ambiguity can be largely reduced by the four-particle cumulant $v_3\{4\}$ measured in experiments. Using the iEBE-VISHNU relativistic viscous hydrodynamic hybrid model simulations with the TRENTo initial condition, we show that solving the v_2 -to- v_3 puzzle and simultaneously describing the $v_3\{4\}$ data in ultracentral $^{208}\text{Pb}+^{208}\text{Pb}$ collisions requires a dynamic octupole deformation with significant fluctuations—a breathing mode of ^{208}Pb around an average octupole shape. Experimental data seem to suggest values of $\langle\beta_3\rangle \sim 0.14$ and $\sigma_{\beta_3} \sim 0.06$. This is the first indication of the octupole vibration/deformation of ^{208}Pb using data from relativistic heavy ion collisions.

In the present study, we implemented a simple Gaussian function for octupole shape fluctuations. However, shape fluctuations characterizing the time-dependent evolution of collective modes in nuclei originate, presumably, from nucleon-nucleon correlations [44, 46]. Realistic nucleon-nucleon correlations exhibit significantly greater complexity than simple Gaussians could capture. Our work can be extended with more realistic profiles of nuclear structure and shape fluctuations. We have employed existing parameter set in our initial-state TRENTo model and final-state iEBE-VISHNU hydrodynamic calculations and applied phenomenological parameterizations for nuclear shape and fluctuations in our present study to compare to experimental data. We have focused only on the v_2/v_3 ratio and ignored the individual v_2 and v_3 magnitudes as they can be tuned by hydrodynamic parameters. However, their tuned values will unlikely be proportional to each other. A full treatment would require Bayesian analysis incorporating nuclear density distributions [69], interplay between shape deformation and fluctuations (demonstrated in this work), hydrodynamic evolution and fluctuations [70], QGP transport properties [71], and technical issues like uncertainties in centrality definitions [72] and estimations of non-collective flow effects [73]. Such an analysis remains a challenge to precisely extract the nuclear shape fluctuations and hydrodynamic parameters of the QGP from relativistic heavy ion collision data. Future improved studies can be built upon our present work and will likely yield further insights into nuclear structure and fluctuations.

The nuclear shape fluctuations investigated in this work may only be discernible in relativistic heavy ion collisions whose yoctosecond timescale ($\sim 10^{-24}$ s) preserves instant states of the nuclear wavefunction as snapshots [74–79]. This allows the identification of the transient “breathing mode”—time-dependent shape distortions—of the colliding nuclei and may enable novel probes of dynamic sub-nuclear structure such as nucleon clustering. Such transient nuclear shapes may not be observable in low-energy nuclear reactions where these fluctuation effects are likely averaged out over the relatively long interaction times ($\sim 10^{-21}$ s) by static equilibrium [80]. This underscores the emerging unique role of relativistic heavy ion collisions in probing novel physics in nuclear structure, complementary to and possibly beyond conventional low-energy

nuclear reactions.

Acknowledgements. We thank Dr. M. Luzum and Dr. X. Wang for useful discussions. This work is supported in part by the National Natural Science Foundation of China under Grants No. 12275082 and No. 12035006 (H.X.), the National Science Foundation under grant number ACI-2004571 within the framework of the XSCAPE project of the JETSCAPE collaboration and by the U.S. Department of Energy, Office of Science, Office of Nuclear Physics, within the framework of the Saturated Glue (SURGE) Topical Theory Collaboration (W.Z.), the National Science Foundation under Grant No. 12247107 and No. 12075007 (X.X., S.Z. and H.S.), and the U.S. Department of Energy under Grant No. DE-SC0012910 (F.W.).

Author contributions. H.X. conceived the idea, designed the study, made the plots, and wrote the initial manuscript; H.X. and W.Z. performed the Trento model simulations; H.X., D.X. and S.Z. performed the hydrodynamic calculations; F.W., H.S., and W.Z. provided critical feedback and revised the manuscript; All authors approved the final version.

Notably concurrent with our arXiv submission, a recent study proposed to resolve the v_2/v_3 puzzle by considering the uniformity of nucleon and sub-nucleon structures in ^{208}Pb [68].

* Corresponding author: haojiexu@zjhu.edu.cn

- [1] M. Gyulassy and L. McLerran, New forms of QCD matter discovered at RHIC, *Nucl. Phys. A* **750**, 30 (2005), arXiv:nucl-th/0405013.
- [2] K. Adcox et al. (PHENIX Collaboration), Formation of dense partonic matter in relativistic nucleus-nucleus collisions at RHIC: Experimental evaluation by the PHENIX collaboration, *Nucl. Phys. A* **757**, 184 (2005), arXiv:nucl-ex/0410003 [nucl-ex].
- [3] B. B. Back et al. (PHOBOS), The PHOBOS perspective on discoveries at RHIC, *Nucl. Phys. A* **757**, 28 (2005), arXiv:nucl-ex/0410022.
- [4] I. Arsene et al. (BRAHMS), Quark gluon plasma and color glass condensate at RHIC? The Perspective from the BRAHMS experiment, *Nucl. Phys. A* **757**, 1 (2005), arXiv:nucl-ex/0410020.
- [5] J. Adams et al. (STAR Collaboration), Experimental and theoretical challenges in the search for the quark gluon plasma: The STAR Collaboration’s critical assessment of the evidence from RHIC collisions, *Nucl. Phys. A* **757**, 102 (2005), arXiv:nucl-ex/0501009 [nucl-ex].
- [6] B. Muller and J. L. Nagle, Results from the relativistic heavy ion collider, *Ann. Rev. Nucl. Part. Sci.* **56**, 93 (2006), arXiv:nucl-th/0602029.
- [7] B. V. Jacak and B. Muller, The exploration of hot nuclear matter, *Science* **337**, 310 (2012).
- [8] P. Braun-Munzinger, V. Koch, T. Schäfer, and J. Stachel, Properties of hot and dense matter from relativistic heavy ion collisions, *Phys. Rept.* **621**, 76 (2016), arXiv:1510.00442 [nucl-th].
- [9] E. Shuryak, Strongly coupled quark-gluon plasma in heavy ion collisions, *Rev. Mod. Phys.* **89**, 035001 (2017), arXiv:1412.8393 [hep-ph].
- [10] S. Acharya et al. (ALICE), The ALICE experiment: a journey through QCD, *Eur. Phys. J. C* **84**, 813 (2024), arXiv:2211.04384 [nucl-ex].

- [11] J.-Y. Ollitrault, Anisotropy as a signature of transverse collective flow, *Phys.Rev.* **D46**, 229 (1992).
- [12] P. F. Kolb and U. W. Heinz, Hydrodynamic description of ultrarelativistic heavy ion collisions, , 634 (2003), [arXiv:nucl-th/0305084](#).
- [13] S. Voloshin and Y. Zhang, Flow study in relativistic nuclear collisions by Fourier expansion of Azimuthal particle distributions, *Z. Phys. C* **70**, 665 (1996), [arXiv:hep-ph/9407282](#).
- [14] U. Heinz and R. Snellings, Collective flow and viscosity in relativistic heavy-ion collisions, *Ann. Rev. Nucl. Part. Sci.* **63**, 123 (2013), [arXiv:1301.2826 \[nucl-th\]](#).
- [15] C. Gale, S. Jeon, and B. Schenke, Hydrodynamic Modeling of Heavy-Ion Collisions, *Int. J. Mod. Phys. A* **28**, 1340011 (2013), [arXiv:1301.5893 \[nucl-th\]](#).
- [16] M. Luzum and H. Petersen, Initial State Fluctuations and Final State Correlations in Relativistic Heavy-Ion Collisions, *J. Phys. G* **41**, 063102 (2014), [arXiv:1312.5503 \[nucl-th\]](#).
- [17] H. Song, Hydrodynamic modelling for relativistic heavy-ion collisions at RHIC and LHC, *Pramana* **84**, 703 (2015), [arXiv:1401.0079 \[nucl-th\]](#).
- [18] S. Jeon and U. Heinz, Introduction to Hydrodynamics, *Int. J. Mod. Phys. E* **24**, 1530010 (2015), [arXiv:1503.03931 \[hep-ph\]](#).
- [19] H. Song, Y. Zhou, and K. Gajdosova, Collective flow and hydrodynamics in large and small systems at the LHC, *Nucl. Sci. Tech.* **28**, 99 (2017), [arXiv:1703.00670 \[nucl-th\]](#).
- [20] R. Derradi de Souza, T. Koide, and T. Kodama, Hydrodynamic Approaches in Relativistic Heavy Ion Reactions, *Prog. Part. Nucl. Phys.* **86**, 35 (2016), [arXiv:1506.03863 \[nucl-th\]](#).
- [21] J. Noronha-Hostler, L. Yan, F. G. Gardim, and J.-Y. Ollitrault, Linear and cubic response to the initial eccentricity in heavy-ion collisions, *Phys. Rev. C* **93**, 014909 (2016), [arXiv:1511.03896 \[nucl-th\]](#).
- [22] J. Noronha, B. Schenke, C. Shen, and W. Zhao, Progress and Challenges in Small Systems, *Int. J. Mod. Phys. E* **33**, 2430005 (2024), [arXiv:2401.09208 \[nucl-th\]](#).
- [23] C. Shen, Z. Qiu, and U. Heinz, Shape and flow fluctuations in ultracentral Pb + Pb collisions at the energies available at the CERN Large Hadron Collider, *Phys. Rev. C* **92**, 014901 (2015), [arXiv:1502.04636 \[nucl-th\]](#).
- [24] K. Aamodt *et al.* (ALICE), Higher harmonic anisotropic flow measurements of charged particles in Pb-Pb collisions at $\sqrt{s_{NN}}=2.76$ TeV, *Phys. Rev. Lett.* **107**, 032301 (2011), [arXiv:1105.3865 \[nucl-ex\]](#).
- [25] G. Aad *et al.* (ATLAS), Measurement of the azimuthal anisotropy for charged particle production in $\sqrt{s_{NN}} = 2.76$ TeV lead-lead collisions with the ATLAS detector, *Phys. Rev. C* **86**, 014907 (2012), [arXiv:1203.3087 \[hep-ex\]](#).
- [26] S. Chatrchyan *et al.* (CMS), Measurement of Higher-Order Harmonic Azimuthal Anisotropy in PbPb Collisions at $\sqrt{s_{NN}} = 2.76$ TeV, *Phys. Rev. C* **89**, 044906 (2014), [arXiv:1310.8651 \[nucl-ex\]](#).
- [27] S. Acharya *et al.* (ALICE), Energy dependence and fluctuations of anisotropic flow in Pb-Pb collisions at $\sqrt{s_{NN}} = 5.02$ and 2.76 TeV, *JHEP* **07**, 103, [arXiv:1804.02944 \[nucl-ex\]](#).
- [28] M. Aaboud *et al.* (ATLAS), Fluctuations of anisotropic flow in Pb+Pb collisions at $\sqrt{s_{NN}} = 5.02$ TeV with the ATLAS detector, *JHEP* **01**, 051, [arXiv:1904.04808 \[nucl-ex\]](#).
- [29] H.-J. Xu, X. Wang, H. Li, J. Zhao, Z.-W. Lin, C. Shen, and F. Wang, Importance of isobar density distributions on the chiral magnetic effect search, *Phys. Rev. Lett.* **121**, 022301 (2018), [arXiv:1710.03086 \[nucl-th\]](#).
- [30] H. Li, H.-j. Xu, Y. Zhou, X. Wang, J. Zhao, L.-W. Chen, and F. Wang, Probing the neutron skin with ultrarelativistic isobaric collisions, *Phys. Rev. Lett.* **125**, 222301 (2020), [arXiv:1910.06170 \[nucl-th\]](#).
- [31] H.-j. Xu, W. Zhao, H. Li, Y. Zhou, L.-W. Chen, and F. Wang, Probing nuclear structure with mean transverse momentum in relativistic isobar collisions, *Phys. Rev. C* **108**, L011902 (2023), [arXiv:2111.14812 \[nucl-th\]](#).
- [32] W. Ryssens, G. Giacalone, B. Schenke, and C. Shen, Evidence of Hexadecapole Deformation in Uranium-238 at the Relativistic Heavy Ion Collider, *Phys. Rev. Lett.* **130**, 212302 (2023), [arXiv:2302.13617 \[nucl-th\]](#).
- [33] H.-j. Xu, J. Zhao, and F. Wang, Hexadecapole Deformation of U238 from Relativistic Heavy-Ion Collisions Using a Nonlinear Response Coefficient, *Phys. Rev. Lett.* **132**, 262301 (2024), [arXiv:2402.16550 \[nucl-th\]](#).
- [34] P. Carzon, S. Rao, M. Luzum, M. Sievert, and J. Noronha-Hostler, Possible octupole deformation of ^{208}Pb and the ultracentral v_2 to v_3 puzzle, *Phys. Rev. C* **102**, 054905 (2020), [arXiv:2007.00780 \[nucl-th\]](#).
- [35] B. G. Zakharov, Collective nuclear vibrations and initial state shape fluctuations in central Pb+Pb collisions: resolving the v_2 to v_3 puzzle, *JETP Lett.* **112**, 393 (2020), [arXiv:2008.07304 \[nucl-th\]](#).
- [36] B. G. Zakharov, Influence of Collective Nuclear Vibrations on Initial State Eccentricities in Pb + Pb Collisions, *J. Exp. Theor. Phys.* **134**, 669 (2022), [arXiv:2112.06066 \[nucl-th\]](#).
- [37] U. W. Heinz and A. Kuhlman, Anisotropic flow and jet quenching in ultrarelativistic U + U collisions, *Phys. Rev. Lett.* **94**, 132301 (2005), [arXiv:nucl-th/0411054](#).
- [38] G. Giacalone, J. Jia, and C. Zhang, Impact of Nuclear Deformation on Relativistic Heavy-Ion Collisions: Assessing Consistency in Nuclear Physics across Energy Scales, *Phys. Rev. Lett.* **127**, 242301 (2021), [arXiv:2105.01638 \[nucl-th\]](#).
- [39] H. Niemi, G. S. Denicol, H. Holopainen, and P. Huovinen, Event-by-event distributions of azimuthal asymmetries in ultrarelativistic heavy-ion collisions, *Phys. Rev. C* **87**, 054901 (2013), [arXiv:1212.1008 \[nucl-th\]](#).
- [40] C. Gale, S. Jeon, B. Schenke, P. Tribedy, and R. Venugopalan, Event-by-event anisotropic flow in heavy-ion collisions from combined Yang-Mills and viscous fluid dynamics, *Phys. Rev. Lett.* **110**, 012302 (2013), [arXiv:1209.6330 \[nucl-th\]](#).
- [41] A. M. Poskanzer and S. A. Voloshin, Methods for analyzing anisotropic flow in relativistic nuclear collisions, *Phys. Rev. C* **58**, 1671 (1998), [arXiv:nucl-ex/9805001](#).
- [42] N. Borghini, P. M. Dinh, and J.-Y. Ollitrault, A New method for measuring azimuthal distributions in nucleus-nucleus collisions, *Phys. Rev. C* **63**, 054906 (2001), [arXiv:nucl-th/0007063](#).
- [43] A. Bilandzic, R. Snellings, and S. Voloshin, Flow analysis with cumulants: Direct calculations, *Phys.Rev.* **C83**, 044913 (2011), [arXiv:1010.0233 \[nucl-ex\]](#).
- [44] P. A. Butler and W. Nazarewicz, Intrinsic reflection asymmetry in atomic nuclei, *Rev. Mod. Phys.* **68**, 349 (1996).
- [45] L. M. Robledo, Enhancement of octupole strength in near spherical nuclei, *Eur. Phys. J. A* **52**, 300 (2016), [arXiv:2003.08122 \[nucl-th\]](#).
- [46] A. Poves, F. Nowacki, and Y. Alhassid, Limits on assigning a shape to a nucleus, *Phys. Rev. C* **101**, 054307 (2020), [arXiv:1906.07542 \[nucl-th\]](#).
- [47] J. M. Yao and K. Hagino, Anharmonicity of multi-octupole-phonon excitations in ^{208}Pb : Analysis with multireference covariant density functional theory and subbarrier fusion of $^{16}\text{O}+^{208}\text{Pb}$, *Phys. Rev. C* **94**, 011303 (2016), [arXiv:1607.02126 \[nucl-th\]](#).
- [48] J. Henderson *et al.*, Deformation and Collectivity in Doubly Magic Pb208, *Phys. Rev. Lett.* **134**, 062502 (2025).
- [49] B.-A. Li, L.-W. Chen, and C. M. Ko, Recent Progress and New

- Challenges in Isospin Physics with Heavy-Ion Reactions, *Phys. Rept.* **464**, 113 (2008), [arXiv:0804.3580 \[nucl-th\]](#).
- [50] C. J. Horowitz and J. Piekarewicz, Neutron star structure and the neutron radius of Pb-208, *Phys. Rev. Lett.* **86**, 5647 (2001), [arXiv:astro-ph/0010227](#).
- [51] M. B. Tsang *et al.*, Constraints on the symmetry energy and neutron skins from experiments and theory, *Phys. Rev. C* **86**, 015803 (2012), [arXiv:1204.0466 \[nucl-ex\]](#).
- [52] D. Adhikari *et al.* (PREX), Accurate Determination of the Neutron Skin Thickness of ^{208}Pb through Parity-Violation in Electron Scattering, *Phys. Rev. Lett.* **126**, 172502 (2021), [arXiv:2102.10767 \[nucl-ex\]](#).
- [53] G. Giacalone, G. Nijs, and W. van der Schee, Determination of the Neutron Skin of Pb208 from Ultrarelativistic Nuclear Collisions, *Phys. Rev. Lett.* **131**, 202302 (2023), [arXiv:2305.00015 \[nucl-th\]](#).
- [54] J. Ritman *et al.*, First observation of the Coulomb-excited double giant dipole resonance in Pb-208 via double-gamma decay, *Phys. Rev. Lett.* **70**, 533 (1993).
- [55] K. Heyde and J. L. Wood, Shape coexistence in atomic nuclei, *Rev. Mod. Phys.* **83**, 1467 (2011).
- [56] H. Song, S. A. Bass, and U. Heinz, Viscous QCD matter in a hybrid hydrodynamic+Boltzmann approach, *Phys. Rev. C* **83**, 024912 (2011), [arXiv:1012.0555 \[nucl-th\]](#).
- [57] C. Shen, Z. Qiu, H. Song, J. Bernhard, S. Bass, and U. Heinz, The iEBE-VISHNU code package for relativistic heavy-ion collisions, *Comput. Phys. Commun.* **199**, 61 (2016), [arXiv:1409.8164 \[nucl-th\]](#).
- [58] J. S. Moreland, J. E. Bernhard, and S. A. Bass, Alternative ansatz to wounded nucleon and binary collision scaling in high-energy nuclear collisions, *Phys. Rev. C* **92**, 011901 (2015), [arXiv:1412.4708 \[nucl-th\]](#).
- [59] J. E. Bernhard, J. S. Moreland, S. A. Bass, J. Liu, and U. Heinz, Applying Bayesian parameter estimation to relativistic heavy-ion collisions: simultaneous characterization of the initial state and quark-gluon plasma medium, *Phys. Rev. C* **94**, 024907 (2016), [arXiv:1605.03954 \[nucl-th\]](#).
- [60] U. W. Heinz, H. Song, and A. K. Chaudhuri, Dissipative hydrodynamics for viscous relativistic fluids, *Phys. Rev. C* **73**, 034904 (2006), [arXiv:nucl-th/0510014](#).
- [61] H. Song and U. W. Heinz, Causal viscous hydrodynamics in 2+1 dimensions for relativistic heavy-ion collisions, *Phys. Rev. C* **77**, 064901 (2008), [arXiv:0712.3715 \[nucl-th\]](#).
- [62] H. Song and U. W. Heinz, Suppression of elliptic flow in a minimally viscous quark-gluon plasma, *Phys. Lett. B* **658**, 279 (2008), [arXiv:0709.0742 \[nucl-th\]](#).
- [63] S. A. Bass *et al.*, Microscopic models for ultrarelativistic heavy ion collisions, *Prog. Part. Nucl. Phys.* **41**, 255 (1998), [*Prog. Part. Nucl. Phys.* 41,225(1998)], [arXiv:nucl-th/9803035 \[nucl-th\]](#).
- [64] M. Bleicher *et al.*, Relativistic hadron hadron collisions in the ultrarelativistic quantum molecular dynamics model, *J. Phys.* **G25**, 1859 (1999), [arXiv:hep-ph/9909407 \[hep-ph\]](#).
- [65] J. S. Moreland, J. E. Bernhard, and S. A. Bass, Bayesian calibration of a hybrid nuclear collision model using p-Pb and Pb-Pb data at energies available at the CERN Large Hadron Collider, *Phys. Rev. C* **101**, 024911 (2020), [arXiv:1808.02106 \[nucl-th\]](#).
- [66] J. Adam *et al.* (ALICE), Centrality Dependence of the Charged-Particle Multiplicity Density at Midrapidity in Pb-Pb Collisions at $\sqrt{s_{\text{NN}}} = 5.02$ TeV, *Phys. Rev. Lett.* **116**, 222302 (2016), [arXiv:1512.06104 \[nucl-ex\]](#).
- [67] J. Adam *et al.* (ALICE), Anisotropic flow of charged particles in Pb-Pb collisions at $\sqrt{s_{\text{NN}}} = 5.02$ TeV, *Phys. Rev. Lett.* **116**, 132302 (2016), [arXiv:1602.01119 \[nucl-ex\]](#).
- [68] Q. Wang, L.-G. Pang, and X.-N. Wang, Impact of Initial-State Nuclear and Sub-Nucleon Structures on Ultra-Central Puzzle in Heavy Ion Collisions, (2025), [arXiv:2504.19208 \[nucl-th\]](#).
- [69] A. V. Giannini, M. N. Ferreira, M. Hippert, D. D. Chinellato, G. S. Denicol, M. Luzum, J. Noronha, T. Nunes da Silva, and J. Takahashi (ExTrEMe), Assessing the ultracentral flow puzzle in hydrodynamic modeling of heavy-ion collisions, *Phys. Rev. C* **107**, 044907 (2023), [arXiv:2203.17011 \[nucl-th\]](#).
- [70] K. Kuroki, A. Sakai, K. Murase, and T. Hirano, Hydrodynamic fluctuations and ultra-central flow puzzle in heavy-ion collisions, *Phys. Lett. B* **842**, 137958 (2023), [arXiv:2305.01977 \[nucl-th\]](#).
- [71] F. G. Gardim, J. Noronha-Hostler, M. Luzum, and F. Grassi, Effects of viscosity on the mapping of initial to final state in heavy ion collisions, *Phys. Rev. C* **91**, 034902 (2015), [arXiv:1411.2574 \[nucl-th\]](#).
- [72] M. Alqahtani, R. S. Bhalerao, G. Giacalone, A. Kirchner, and J.-Y. Ollitrault, Impact parameter dependence of anisotropic flow: Bayesian reconstruction in ultracentral nucleus-nucleus collisions, *Phys. Rev. C* **110**, 064906 (2024), [arXiv:2407.17308 \[nucl-th\]](#).
- [73] Y. Feng and F. Wang, Review of nonflow estimation methods and uncertainties in relativistic heavy-ion collisions, *J. Phys. G* **52**, 013001 (2025), [arXiv:2407.12731 \[nucl-ex\]](#).
- [74] A. Dimri, S. Bhatta, and J. Jia, Impact of nuclear shape fluctuations in high-energy heavy ion collisions, *Eur. Phys. J. A* **59**, 45 (2023), [arXiv:2301.03556 \[nucl-th\]](#).
- [75] G. Giacalone *et al.*, The unexpected uses of a bowling pin: exploiting ^{20}Ne isotopes for precision characterizations of collectivity in small systems, (2024), [arXiv:2402.05995 \[nucl-th\]](#).
- [76] M. I. Abdulhamid *et al.* (STAR), Imaging shapes of atomic nuclei in high-energy nuclear collisions, *Nature* **635**, 67 (2024), [arXiv:2401.06625 \[nucl-ex\]](#).
- [77] S. Zhao, H.-j. Xu, Y. Zhou, Y.-X. Liu, and H. Song, Exploring the Nuclear Shape Phase Transition in Ultra-Relativistic $^{129}\text{Xe}+^{129}\text{Xe}$ Collisions at the LHC, *Phys. Rev. Lett.* **133**, 192301 (2024), [arXiv:2403.07441 \[nucl-th\]](#).
- [78] G. Giacalone *et al.*, Anisotropic Flow in Fixed-Target Pb208+Ne20 Collisions as a Probe of Quark-Gluon Plasma, *Phys. Rev. Lett.* **134**, 082301 (2025), [arXiv:2405.20210 \[nucl-th\]](#).
- [79] H. Mäntysaari, B. Schenke, C. Shen, and W. Zhao, Probing nuclear structure of heavy ions at energies available at the CERN Large Hadron Collider, *Phys. Rev. C* **110**, 054913 (2024), [arXiv:2409.19064 \[nucl-th\]](#).
- [80] C. Simenel, K. Godbey, and A. S. Umar, Timescales of quantum equilibration, dissipation and fluctuation in nuclear collisions, *Phys. Rev. Lett.* **124**, 212504 (2020), [arXiv:2005.04357 \[nucl-th\]](#).